Articles

SSZ-51—A New Aluminophosphate Zeotype: Synthesis, Crystal Structure, NMR, and Dehydration Properties

Russell E. Morris,*,† Allen Burton,‡ Lucy M. Bull,‡ and Stacey I. Zones‡

School of Chemistry, University of St Andrews, Purdie Building, St Andrews, KY16 9ST, U.K., and ChevronTexaco Energy Research and Technology Company, Richmond, California 94802

Received December 10, 2003. Revised Manuscript Received March 31, 2004

A new aluminophosphate zeotype framework structure, SSZ-51 ($Al_4(PO_4)_4F.C_7N_2H_{11}\cdot 0.5H_2O$), has been prepared in the presence of 4-dimethylaminopyridine as a structure-directing agent and a fluoride ion-mineralizing agent. The structure of the material was solved using single-crystal X-ray diffraction at a synchrotron source. It is closely related to the structure of SAPO-40 (AFR) and contains intersecting channels delimited by 8- and 12-membered ring windows. The occluded structure-directing agent and fluoride can be calcined to yield a material with appreciable microporosity. The calcination and dehydration of SSZ-51 was followed using variable temperature synchrotron X-ray powder diffraction and showed that the adsorption of water at low temperatures leads to a loss in long-range order of the framework. The long-range order of the framework is regained by dehydration at temperatures above 100 °C.

Introduction

Zeolites and microporous materials (zeoltypes) make up an important family of solids, with well-known applications in ion exchange and gas separation. In addition, they are set to become important in new technologies as they are increasingly of interest for emerging applications in a wide range of areas.[1] The applications of zeotypes are often intimately connected with their structure. Their open structures give rise to high surface areas and the narrow pore size distributions can produce some interesting selectivity effects. In addition, there are many different elements that can be incorporated into the frameworks, so allowing control over the chemical properties of the materials. Aluminophosphates ($AlPO_4$) make up an important member of this family of materials. Hydrothermal synthesis has been used to crystallize a large variety of open framework aluminophosphates since the initial reports of the AlPO-*n* series in the early 1980s.[2] In the past decade the use of fluoride ions as mineralizing agents in the synthesis of new microporous materials has developed considerably.[3,4] They have been used to great effect to prepare many new framework structures, including pure silica and aluminosilicate zeolites, aluminophosphates, and gallium phosphates.[5,6] The major advantages of the fluoride route, which was pioneered by Flanigen and Patton,[7] is that the solids are relatively defect-free,[8] they are generally low density, and they can be grown as quite large crystals.[9] The lack of defects in a zeolite can have major effects on the hydrophobicity of the material, which can be important in catalytic applications. Fluoride ions have three primary roles in the synthesis of framework structures: a mineralizing role in improving the solubility of the ions that will condense to form the framework at neutral or acidic pHs, a catalytic role in the formation of bonds in the materials and a charge-balancing role, and providing a negative charge to the framework that balances the positive charge on any occluded cationic structure-directing agents (SDAs).[10,11,12] When acting to charge-balance the organic SDAs, the fluoride ions show different properties from other methods of introducing a negative ion into the framework. In aluminophos-

* To whom correspondence should be addressed.
† University of St Andrews.
‡ ChevronTexaco Energy Research and Technology Company.

(1) Davis, M. E. *Nature* **2002**, *417*, 813−821.
(2) Wilson, S. T.; Lok, B. M.; Messina, C. A.; Cannon, T. R.; Flanigen, E. M. *J. Am. Chem. Soc.* **1982**, *104*, 1146.
(3) Kessler, H.; Patarin, J.; Schottdarie, C. *Stud. Surf. Sci. Catal.* **1994**, *85*, 75.
(4) Cundy, C. S.; Cox, P. A. *Chem. Rev* **2003**, *103*, 663.
(5) (a) Gougeon, R. D.; Brouwer, E. B.; Bodart, P. R.; Delmotte, L.; Marichal, C.; Chezeau, J. M.; Harris, R. K. *J. Phys. Chem. B* **2001**, *105*, 12249. (b) Wheatley, P. S.; Morris, R. E. *J. Solid State Chem.* **2002**, *167*, 267.
(6) Sassoye, C.; Marrot, J.; Loiseau, T.; Férey, G. *Chem. Mater.* **2002**, *14*, 1340.
(7) Flanigen, E. M.; Patton, R. L. U.S. Patent 4073865, 1978.
(8) Camblor, M. A.; Villaescusa, L. A.; Diaz-Cabanas, M. J. *Top. Catal.* **1999**, *9*, 59.
(9) Kuperman, A. S.; Oliver, S.; Ozin, G. A.; Garces, J. M.; Olken, M. M. *Nature* **1993**, *365*, 239.
(10) Barrett, P. A.; Camblor, M. A.; Corma, A.; Jones, R. H.; Villaescusa, L. A. *J. Phys. Chem. B* **1998**, *102*, 4147.
(11) Villaescusa, L. A.; Wheatley, P. S.; Bull, I.; Lightfoot, P.; Morris, R. E. *J. Am. Chem. Soc.* **2001**, *123*, 8797.
(12) Akporiaye, D. E.; Fjellvag, H. Halvorsen, E. N.; Haug, T.; Karlsson, A.; Lillerud, K. P *Chem. Commun.* **1996**, 1553.

10.1021/cm0353005 CCC: $27.50 © 2004 American Chemical Society
Published on Web 06/26/2004

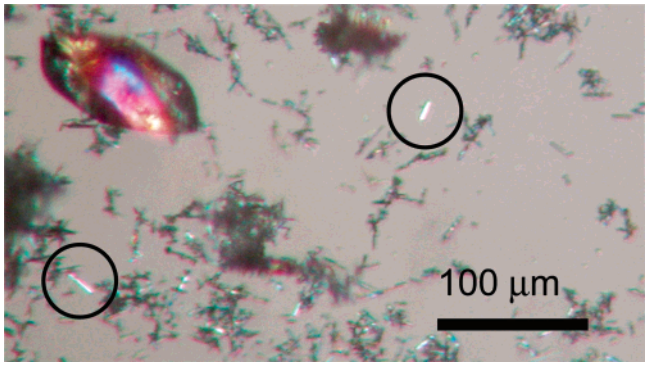

Figure 1. Optical polarizing micrograph of the crystals of SSZ-51 (larger examples are circled) compared in size to that of berlinite crystals (top left-hand corner), which is a minor impurity in the preparation that contained the crystals used in the X-ray structural study.

phates the negative charge can be introduced by substituting silicon for a phosphorus atom to form a silico aluminophosphate (SAPO) or by substituting a divalent metal cation for some of the Al^{3+} cations to form a metal aluminophosphate (MeAPO). The addition of fluoride ions to the framework, however, produces a "harder" negative charge as it is closely associated with the fluoride ion rather than being spread around the four oxygen atoms that surround an aliovalent substituting cation. This, coupled with the fact that the incorporation of fluoride ions into the framework is often more favorable at certain specific sites, leads to strong interaction with the SDA and some interesting effects, including the non-centrosymmetric ordering of the SDA even though the framework itself is centrosymmetric.[13]

In this paper we report the synthesis, crystal structure determination, and calcination/dehydration behavior of the novel aluminophosphate zeolite, SSZ-51 ($Al_4(PO_4)_4F.C_7N_2H_{11}\cdot 0.5H_2O$). We discuss the close structural relationship between this material and zeolite AFR (SAPO-40).[14]

Experimental Section

Synthesis. A sample of SSZ-51 was synthesized as follows. In the Teflon cup (23-mL size) of a Parr Chemical Co. stainless steel reactor, we mixed into 9 mL of water the following reagents: 2.2 g of 85% phosphoric acid, 0.22 g of hydrofluoric acid (50%), 0.90 g of 4-dimethylaminopyridine (DMAP; caution: highly toxic), and 1.33 g of APO-208 pseudoboehmite alumina (74% Al_2O_3). The reactor was closed up and heated for 2 days at 180 °C without stirring. Collection of the white solid by recovery and washing of the solids formed via filtration yielded SSZ-51 with the chemical formula $Al_4(PO_4)_4F\cdot C_7N_2H_{11}\cdot 0.5H_2O$. The reaction can also be carried out in the presence of a silicon source (0.06 g of Cabosil M-5 fumed silica) to produce a siliconaluminophosphate with the same framework. Some preparations yielded a small amount of berlinite as an impurity (Figure 1), and the sample used for single-crystal and variable temperature X-ray diffraction did contain a very small amount of the impurity. However, other samples prepared were pure phases of either the AlPO or SAPO versions of SSZ-51. Chemical analysis by ICP confirms the presence of fluorine in the structure as does ^{19}F MAS NMR (chemical shift, −100 ppm). The level of fluorine incorporation (1.9 wt %) is slightly lower than that expected from the chemical formula (2.5%) and a small amount of F/OH disorder in the framework cannot be ruled out. It should be noted however that fluoride is necessary for the reaction to produce SSZ-51.

Table 1. Crystal Data and Structure Refinement for SSZ-51

empirical formula	$Al_4(PO_4)_4F\cdot C_7N_2H_{11}\cdot 0.5H_2O$
formula weight	637.97
temperature	150(2) K
wavelength	0.6875 Å
crystal system, space group	monoclinic, *C*2/*c*
unit cell dimensions	$a = 21.759(3)$ Å
	$b = 13.8214(18)$ Å, $\beta = 98.849(4)°$
	$c = 14.2237(18)$ Å
volume	4226.7(9) Å^3
Z, calculated density	8, 2.005 Mg/m^3
absorption coefficient	0.62 mm^{-1}
F(000)	2560
crystal size	0.03 × 0.01 × 0.005 mm
θ range for data collection	1.89−30.47°
reflections collected/unique	8454/5039 [*R*(int) = 0.0519]
absorption correction	none
refinement method	full-matrix least-squares on F^2
data/restraints/parameters	5039/0/315
goodness-of-fit on F^2	1.012
final *R* indices [$I > 2\sigma(I)$]	R1 = 0.0629, wR2 = 0.1445
R indices (all data)	R1 = 0.1119, wR2 = 0.1647
largest diff. peak and hole	0.895 and −0.618 e·A^{-3}

A pure sample of product SSZ-51 was calcined to 540 °C in a mixture of nitrogen gas with about 2% air mixed in. The sequence was to heat to 120 °C at 1 °C/min, then hold for 3 h at that temperature, then heat at 1 °C/min to 540 °C, and hold for 3 h. Upon cooling, the solid had lost 23.6 wt %. The sample was kept relatively free from water and then reheated to 400 °C as a pretreatment for determination of micropore volume by pore-filling with argon. The micropore volume was determined to be about 25 wt % for argon at 87 K. The crystals are large enough that this value constitutes almost the entire pore volume for the sample.

Single-Crystal X-ray Diffraction. Figure 1 shows the sample of SSZ-51 viewed under a polarizing optical microscope. The large crystals are berlinite ($AlPO_4$), a dense phase impurity that is present in very small quantities in the sample that contains the best single crystals of SSZ-51. The small single crystals of about 20−30 μm in length exhibited bright faces and extinguished polarized light in a manner that suggested they were all reasonably high quality single crystals. One crystal of approximate size 30 × 10 × <5 μm was mounted on the end of a small piece of glass wool (itself glued to a larger glass capillary) using a fluoropolyether "oil". This was then mounted onto the diffractometer. Diffraction data were collected using X-rays of wavelength 0.6875 Å (Silicon 111 monochromator) on a Bruker-Nonius goniometer equipped with a 1 K CCD area detector at the Synchrotron Radiation Source at the Daresbury Laboratories, U.K. The temperature was held at 150 K.

As expected for a smallish crystal, the diffraction intensity was relatively weak. However, the diffraction spots were relatively sharp (rocking curve width ~0.4°). Details of the structure solution and refinement are given in Table 1 and the Supporting Information. Structure solution was carried out using the program SHELXS-97 and least-squares refinement using the program SHEXL-97. The structure was solved using the normal procedures, with all the framework atoms found from the Direct Methods and the remaining atoms found from subsequent difference Fourier syntheses. The organic structure-directing agent (SDA) was located and refined successfully as 4-dimethylaminopyridinium. Hydrogen atoms were placed in geometrically sensible positions on the pyridine ring and refined as "riding atoms" on the carbon/nitrogen atoms to which they were connected (i.e., their positions are recalculated at the end of each cycle of refinement). A difference Fourier map of the region where possible methyl hydrogens could sit was calculated, and one hydrogen atom was

(13) Bull, I.; Villaescusa, L. A.; Teat, S. J.; Camblor, M. A.; Wright, P. A.; Lightfoot, P.; Morris, R. E. *J. Am. Chem. Soc.* **2000**, *122*, 7128.
(14) (a) Estermann, M. A.; McCusker, L. B.; Baerlocher, Ch. *J. Appl. Crystallogr.* **1992**, *25*, 539. (b) Ramaswamy, V.; McCusker, L. B.; Baerlocher, Ch. *Microporous Mesoporous Mater.* **1999**, *3*, 1.

placed at the maximum value of the electron density. The others were then placed to complete the tetrahedron around the methyl carbon. The torsion angles defining the positions of the hydrogen atoms relative to the methyl carbon were then refined.

Near the end of the refinement procedure the top three difference Fourier peaks were in positions that could be occupied by the oxygen atoms of water molecules. These atoms were included in the model and refined successfully as approximately 0.5 water molecules per asymmetric unit (4 water molecules per unit cell). This agrees closely with thermogravimmetric analysis; the sample lost 1.8 wt % from room temperature to 175 °C and then lost 20.9 wt % from ~200 to 350 °C (calculated loss of water = 1.4%, calculated loss of SDA = 19.3%).

The final cycles of least-squares refinement contained anisotropic displacement parameters for the framework atoms and the carbon and nitrogen atoms of the SDA. The hydrogen atom isotropic displacement parameters were fixed at 1.2 times the *U*(eq) of the atom to which they were attached. The oxygen atoms of the water molecules were refined with isotropic displacement parameters. The hydrogen atoms of the water molecules were not located.

Given the relationship between SSZ-51 and AFR described below, twinning is always a possibility. However, no evidence for this was found when the twin laws were tested in the refinement.

Powder X-ray Diffraction. The as-made sample of SSZ-51 was packed in an *unsealed* 1-mm outer diameter quartz capillary. The capillary was then mounted in a heating stage at beamline X7A at the National Synchrotron Light Source, Brookhaven, Upton, NY. Data were collected at wavelength λ = 0.70387 Å, and intensities were monitored with a PSD detector. The sample was heated in open air in 100 °C increments up to 800 °C. After completion of the initial series of experiments to remove the organic, the material was removed from the glass capillary and placed over a beaker containing water. After the material was allowed to hydrate for a day, the sample was then loaded back into another capillary and data were again collected in 100 °C increments.

Magic Angle Spinning NMR. NMR spectra were collected on Bruker DSX and Avance 500 spectrometers using 4-mm double-resonance Bruker MAS probes. The samples were spun at the magic angle at 10−12 kHz. ^{31}P NMR spectra were collected with proton decoupling using a relaxation time of 60 s and a 4-μs excitation pulse. Spectra were referenced to 85% H_3PO_4 at 0 ppm.^{27}Al NMR spectra were collected with ^{1}H decoupling using a 2-μs pulse and a relaxation delay of 1 s. The spectra were referenced to $Al(NO_3)_3$ at 0 ppm. 2D ^{27}Al NMR MQMAS spectra were collected using the z-filter pulse sequence proposed by Amoureux et al.[15] The pulse lengths were optimized on the sample and were found to be 4.4 and 1.6 μs for the first and second pulses, respectively. The selective 90° pulse was 25 μs. The data were processed using the States method to obtain pure-phase spectra. The spectrum of dehydrated SSZ-51 was collected on a sample that had previously been heated at 115 °C for 48 h. The sample was packed in air, but was spun in N_2. The rehydrated sample was obtained after exposing the dehydrated sample to air saturated with water for at least 12 h. The sample was not found to rehydrate or dehydrate while spinning in unsealed rotors under N_2 in the NMR magnet.

Results and Discussion

The framework structure of SSZ-51 consists of the building unit shown in Figure 2, which is essentially a double four ring (D4R) with one disconnected (or ring-opened) edge. The fluoride ion is encapsulated within this building unit and forms a bridge between two of the aluminum atoms (Al6 and Al7). This produces two types of aluminum in the structure, as shown in Figure 2. Al5 and Al8 are tetrahedrally coordinated by four oxygen atoms while the Al6 and Al7 form trigonal bipyramidal AlO_4F units, and the structure contains an Al−F−Al link. The bond distances and angles around each of the aluminum and phosphorus atoms in the structure are consistent with those expected for the types of unit in which they are contained. Each building unit is then connected to four other identical building units, through two Al−O−P linkages per unit. Figure 3 shows how these building units can be linked together to form the two very closely related structures, the SSZ-51 structure reported here and AFR.[14] In both SSZ-51 and AFR the building units (Figure 2) are joined in a "head-to-tail" fashion to form chains running parallel to the *c*-direction. The chains are linked together through four-rings to form undulating layers where the orientation of successive chains in these layers is antiparallel. This layer is a building block of both SSZ-51 and AFR. The undulating layers can be linked in two ways. If the layers are linked so that there is inversion symmetry between the layers, this results in the SSZ-51 structure. If the layers are linked so that there is "mirror" symmetry between the layers, the resulting structure is that of AFR (mirror symmetry here refers to the framework, i.e., excludes the need for Al/P ordering). An alternative description is that the successive layers in the SSZ-51 framework are related by a translation of $^1/_2(a + b)$ while successive layers in AFR framework are related by a translation of $^1/_2(a + b)$ + 2-fold rotation around *a*.

The differences in symmetry (monoclinic *C*2/*c* for SSZ-51 and orthorhombic *Pmmn* for AFR) between the two

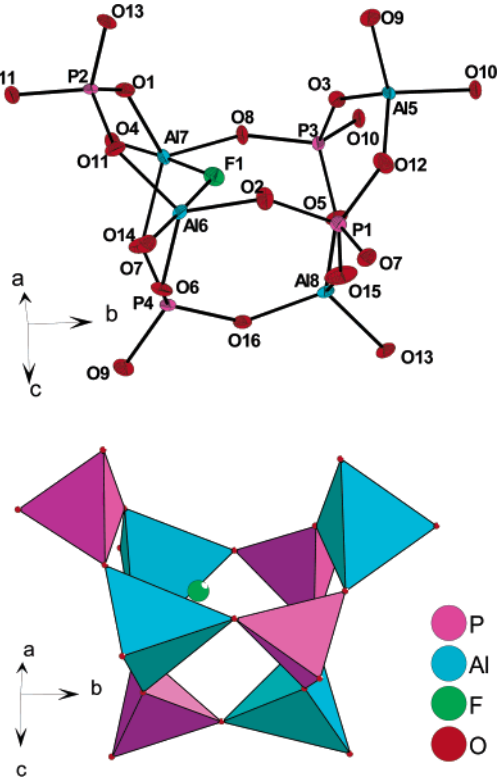

Figure 2. Two views of the "ring-opened D4R" unit showing the atom numbering scheme and the location of the fluoride ion. Thermal ellipsoids are set at 50%.

(15) Amoureux, J. P.; Fernandez, C *Solid State Magn. Res.* **1998**, *10*, 211.

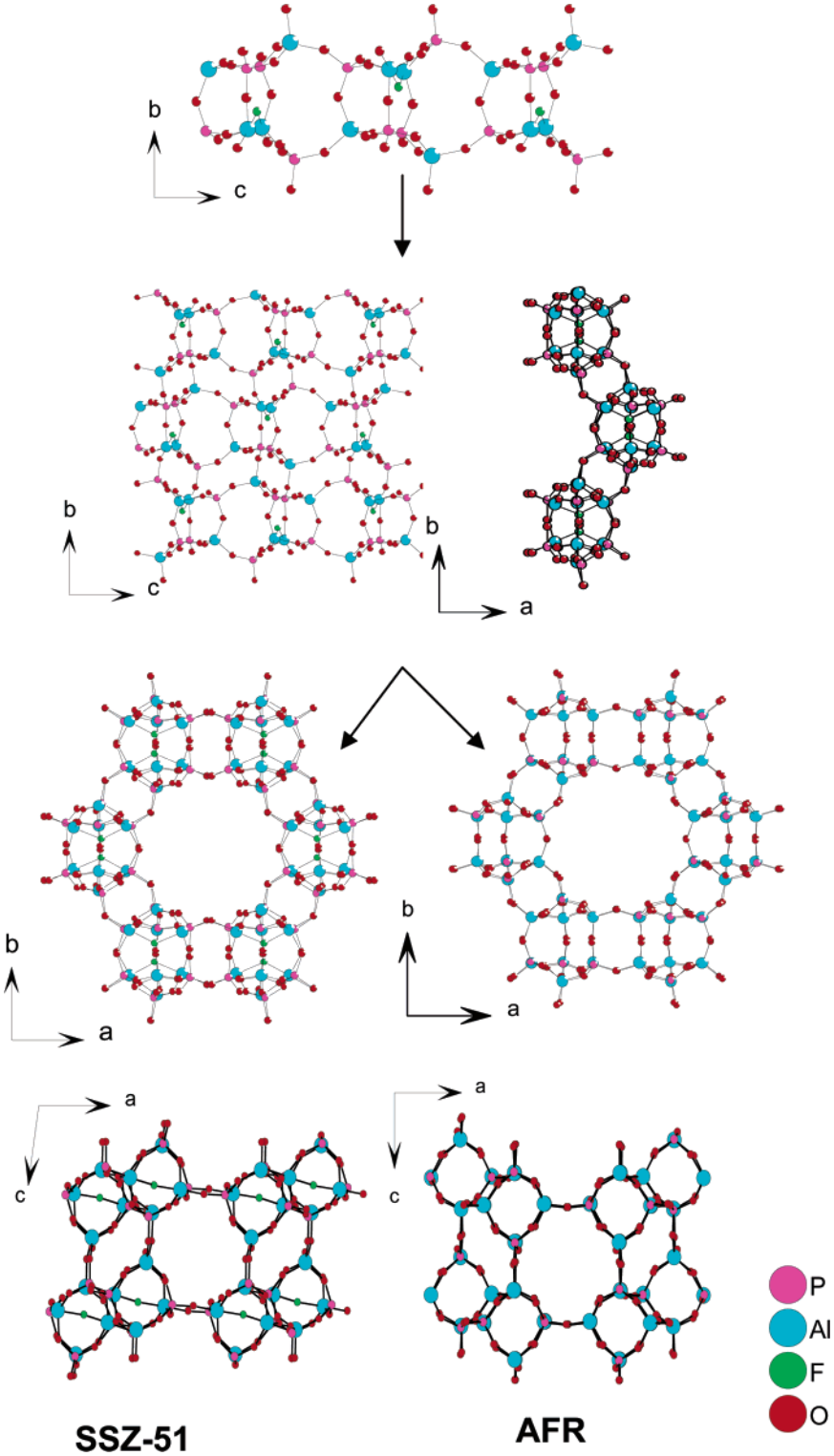

Figure 3. Building scheme showing the relationship between the SSZ-51 and AFR structures. In both structures the building units shown in Figure 2 are linked "head to tail" into chains. These chains are linked to form undulating layers. The layers can be further linked in two different ways: via inversion symmetry to form SSZ-51 (left) and via mirror symmetry to form AFR (right). The easiest projection to see the difference in the two structures is parallel to the *b*-axis.

structures are significant in that they lead to completely different atomic connectivity. (Note that there is still some controversy regarding the actual space group symmetry of AFR, especially with respect to the explanation of MAS NMR results,[16] since the structure has only been solved from powder X-ray diffraction but the atomic connectivity of the AFR is well-defined from the work of Baerlocher and co-workers[14]). However, the overall channel structures of the two materials SSZ-51 and AFR look almost identical and it is difficult to tell them apart by only looking at projections of the structure, especially the projection viewed parallel to the

(16) Fernandez, C.; Morais, C.; Rocha J.; Pruski, M. *Solid State Nucl. Magn. Reson.* **2002**, *21*, 61.

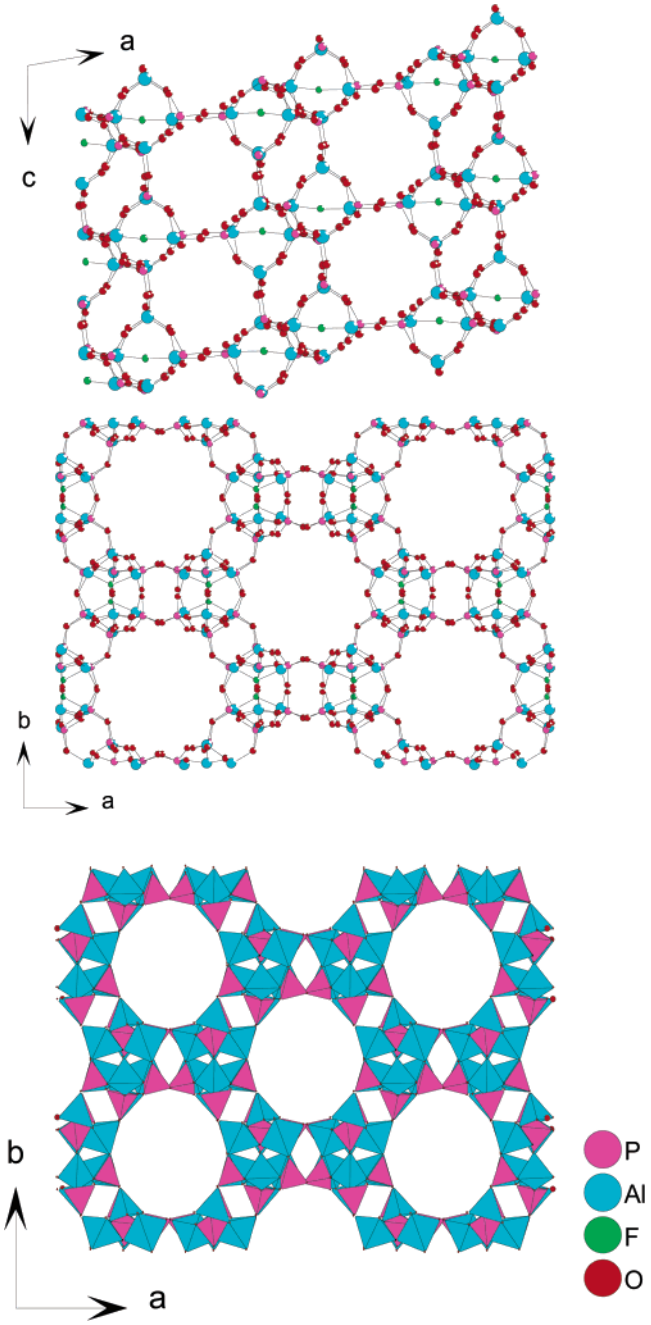

Figure 4. Two channels present in the SSZ-51 framework. The 8MR channel (top) and the 12MR channel (middle). The bottom view is a polyhedral representation of the structure viewed parallel to 12MR channels (purple = PO_4, cyan = AlO_4 and AlO_4F).

largest channels in the structure. The building scheme (Figure 3) helps to visualize the difference between the two structures, and the easiest direction to view the differences between the two structures is the view parallel to the *b*-axis, where it is relatively easy to see the origins of the monoclinic symmetry of SSZ-51 and the orthorhombic symmetry of the AFR framework.

The overall structure of SSZ-51 consists of a two-dimensional intersecting channel system (Figure 4). One of the channels runs parallel to the crystallographic *b*-axis and is defined by an 8-membered ring window (8MR, a window defined by eight tetrahedral units). Perpendicular to this channel and running parallel to the crystallographic *c*-axis is a larger channel defined

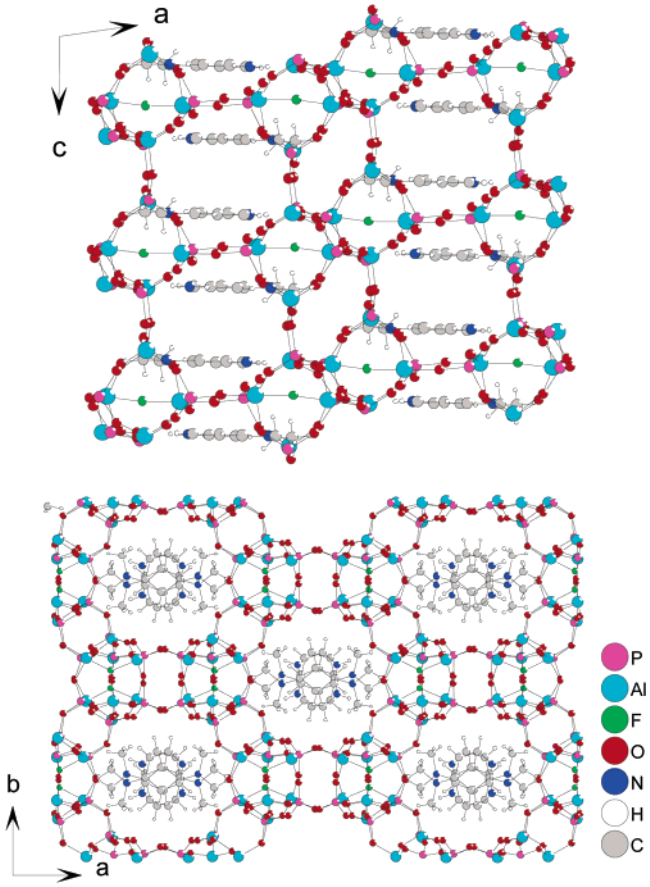

Figure 5. Views of the structure of SSZ-51 showing the location of the SDA in relation to the 12- and 8-membered rings.

by a 12-membered ring. This is essentially the same channel structure as AFR. The ZON[17] framework also contains the ring-opened D4R unit, but this is connected in a different way to produce two 8-ring channels.

The close similarity between the channel structures and unit cells of SSZ-51 (a = 21.759(3) Å, b = 13.8214(18) Å, c = 14.2237(18) Å, β = 98.849(4)°, $\alpha = \gamma = 90°$) and AFR (a = 21.944 Å, b = 13.691 Å, c = 14.249 Å, $\alpha = \beta = \gamma = 90°$) despite their different atomic connectivity offers a warning that phase identification is not always as straightforward as it might appear, especially if only powder X-ray diffraction data are available and great care must be taken to ensure that the correct symmetry is identified.

Figure 5 shows the overall view of the SSZ-51 structure itself, illustrating the location of the SDAs inside the 12-ring channels. Figure 6 then shows a close-up of the SDA location including the possible hydrogen bond (d(H...O) = 2.00 Å) between the protonated nitrogen of the 4-dimethylaminopyridine and the oxygen (O11) of the framework. Note that O11 is part of the AlO_4F unit and is therefore spatially close to the negative charge on the framework. The orientation of the SDA inside the pores of SSZ-51 is probably controlled by the electrostatic interactions between the relatively hard negative charge on the fluoride and the positive charge of the pyridinium group, coupled with

(17) (a) Marler, B.; Patarin, J.; Sierra, L. *Microporous Mater.* **1995**, *5*, 151. (b) Akporiaye, D. E.; Fjellvag, H.; Halvorsen, E. N.; Hustveit, J.; Karlsson, A.; Lillerud, K. P. *Chem. Commun.* **1996**, 601.

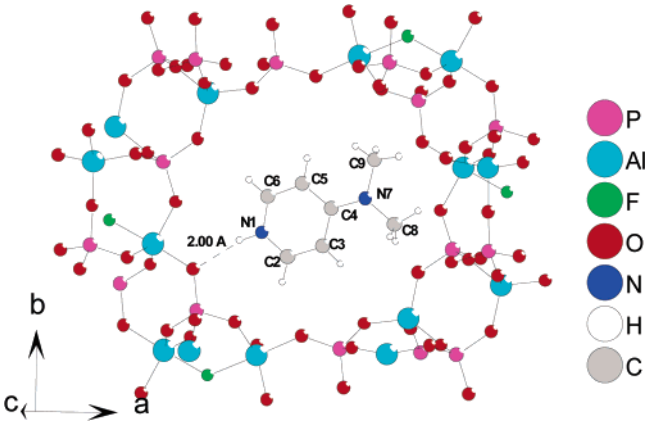

Figure 6. Location and numbering scheme of the SDA and its position in relation to the 12MR window in the SSZ-51 structure. The possible hydrogen bond is shown as a dashed line.

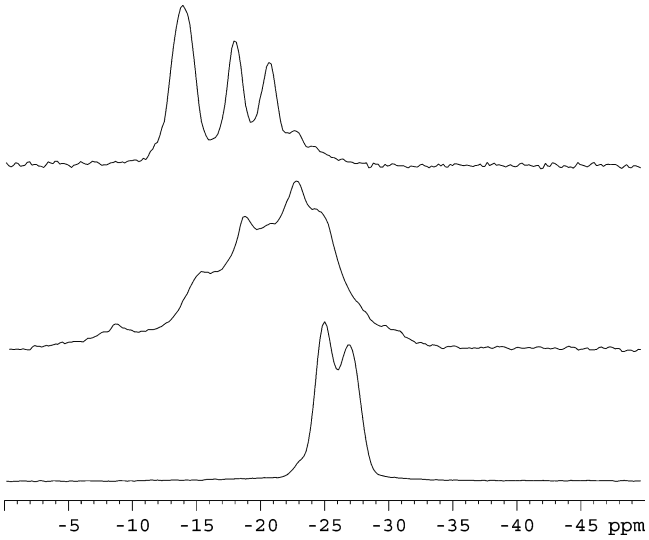

Figure 7. ^{31}P MAS NMR spectra of templated, hydrated, and dehydrated SSZ-51 (top to bottom). The spectra were collected at the California Institute of Technology at 11.7 T using ^{1}H decoupling during the acquisition. The spectra were referenced to 85% H_3PO_4 at 0 ppm.

the long hydrogen bond. A similar situation is found when 4-dimethylaminopyridine has been used in the synthesis of a layered fluoride-containing gallium phosphate.[18] The gallium phosphate has the same building unit as SSZ-51, but the connectivity of the units is such that flat layers are produced. The nitrogen of the SDA is H-bonded to an oxygen atom of the GaO_4F unit in a similar way to that in SSZ-51. The fluoride ion occupies almost the same position as the fluoride in SSZ-51. A similar bridging position is taken up by hydroxide in the AlPO-40 version of AFR.[14b]

NMR Experiments. We also performed ^{31}P MAS NMR and ^{27}Al MAS NMR experiments on the calcined, as-made (templated), dehydrated, and rehydrated materials. Figure 7 shows the ^{31}P magic angle spinning (MAS) NMR of a pure sample of templated, calcined, and hydrated SSZ-51. The peaks in the ^{31}P NMR spectrum of the calcined material around −25 to −30 ppm are in a spectral range consistent with other open framework aluminum phosphates reported in the literature. The ^{31}P NMR spectrum of the as-made material shows three major resolved peaks, which have relative intensities of 2:1:1, suggesting that there are at least three distinct phosphorus sites in the crystal structure. The crystal structure (Figure 2) shows that there are four crystallographically independent phosphorus sites. Two of these are close to the fluoride ions and two further away from the fluorides. The spectrum can therefore be explained by two unresolved phosphorus resonances of one type and two resolved resonances of the other, which is consistent with the crystal structure. In addition to the major peaks, there also appears to be visible resonances of low intensity at around −25 ppm. The origin of these small resonances is not certain at the present time but they may be related to the fact that elemental analysis seems to suggest that some fluoride sites may be occupied by hydroxide. This would lead to a small percentage of phosphorus atoms being in the vicinity of Al−OH−Al rather than Al−F−Al linkages, which would lead to a slightly different NMR spectrum.

Upon calcination and dehydration, the ^{31}P spectrum shows two resolved resonances. Calcination will remove the organic structure-directing agent and the fluorine from the framework and leave just tetrahedral aluminum and phosphorus. The absence of fluoride in the calcined structure means that the phosphorus atoms are all now in more similar local environments to each other than they were in the as-made materials. However, the symmetry of the material indicates that unless there has been a transformation from monoclinic to orthorhombic (which the variable temperature XRD reported below shows is not the case), then the two visible resonances must contain signals from four independent phosphorus atoms.

Upon rehydration (Figure 7), the ^{31}P MAS NMR spectrum shows several broad resonances, consistent with further interaction of the framework atoms with water. This observation is also consistent with the apparent lack of long-range order from the powder XRD pattern of the hydrated material (see Figure 11). This is probably caused by the water disrupting the framework by forming octahedral species similar to that seen previously in samples of AFR. A full determination of the mode of action of water will require a much more detailed NMR study similar to those that have been carried out on AlPO-40[16] and SAPO-40,[19] both of which have the AFR framework structure, but it is clear that this framework is somewhat unstable with regard to hydration. The ^{31}P spectrum of further dehydrated SSZ-51 is similar to the spectrum of the calcined material, indicating that the reactions on contact with water are reversible.

The ^{27}Al NMR spectrum of the templated SSZ-51 (Figure 8) shows peaks in shift ranges that correspond to 4- and 5-coordinated aluminum (∼40 and ∼20 ppm, respectively) consistent with the crystal structure of SSZ-51. The aluminum atoms bonded to fluoride give rise to the resonance at 20 ppm. After calcination and dehydration, the aluminum is 4-coordinate.

(18) Wragg, D. S.; Morris, R. E. *J. Phys Chem. Solids* **2001**, *62*, 1493.

(19) Lourenco, J. P.; Ribeiro, M. F.; Ribeiro, F. R.; Rocha, J.; Gabelica, Z.; Derouane, F. G. *Microporous Mater.* **1995**, *4*, 445.

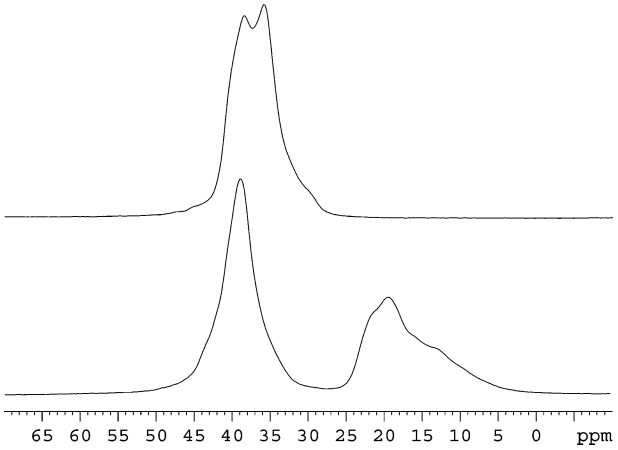

Figure 8. ^{27}Al MAS NMR spectra of SSZ-51 templated (bottom) and calcined (top). The spectra were collected at the California Institute of Technology at 11.7 T using ^{1}H decoupling during the acquisition. The spectra were referenced to $Al(NO_3)_3$ at 0 ppm.

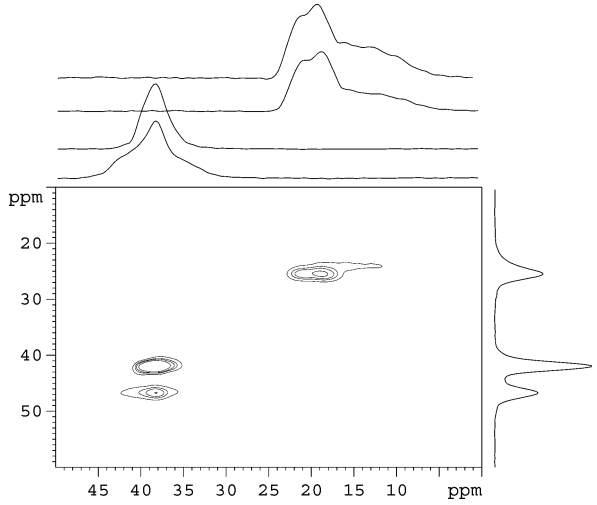

Figure 9. ^{27}Al 2D MQMAS NMR spectra of templated SSZ-51. The spectrum was collected at the California Institute of Technology at 11.7 T using ^{1}H decoupling during the acquisition. The spectra were referenced to $Al(NO_3)_3$ at 0 ppm. The spectra along the *y*-axes are the projections across the 2D plot showing the high-resolution spectra without the broadening from the quadrupolar interaction. The projections in the vertical direction are shown along the *x*-axis. These are the MAS line shapes for each of the resolved peaks in the horizontal projection. These line shapes can be simulated to obtain the quadrupolar interaction, which can then be related to the local symmetry of the Al site.

Since ^{27}Al is a quadrupolar nucleus, magic angle spinning does not give the highest resolution spectrum possible as the second-order anisotropic quadrupolar interaction is not fully averaged. Multiple quantum magic angle spinning (MQMAS) allows distinct Al sites to be distinguished using a conventional MAS NMR probe. Figure 9 shows MQMAS spectra of the as-made sample of SSZ-51. The 2D^{27}Al MQMAS spectrum was obtained from the as-made SSZ-51. At least two tetrahedral and two pentacoordinate sites are observed; again, this is consistent with the X-ray diffraction as from the single-crystal structure we know that there are two distinct tetrahedrally coordinated Al sites and two distinct pentacoordinated sites. Again, even though the resolution in the ^{31}P NMR spectrum is not sufficient, a structural model with four Al and four P sites all of the same occupancy is consistent with the spectra.

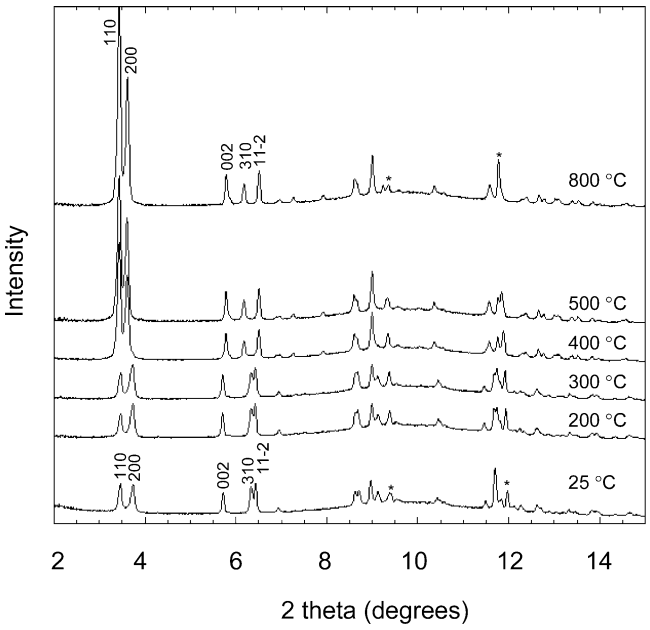

Figure 10. Variable temperature X-ray diffraction during the calcination of SSZ-51 (∗ mark the positions of peaks from the berlinite impurity).

The room temperature powder X-ray diffraction (XRD) pattern of SSZ-51 changes dramatically after calcination to remove the occluded organic template and fluoride ions. There seems to be a distinct loss of crystallinity, with diffraction peaks for the calcined sample being much broader and less well-defined than for the uncalcined sample. At first glance it seems that the calcination procedure has probably resulted in some breakdown of the framework structure. However, calcined SSZ-51 possesses appreciable microporosity (close to FAU-type zeolites), and density functional theory (DFT) simulations[20] of the microporosity results indicated the likely presence of 12- and 8-rings. This is consistent with the removal of fluoride and structure-directing agent while retaining the framework structure intact. These two results are therefore seemingly at odds. To follow the calcinations process, we collected variable temperature powder X-ray diffraction data on the as-made sample at the NSLS synchrotron source in Brookhaven in order to monitor structural changes as SSZ-51 is heated in air.

Figure 10 shows the effect of temperature on the powder diffraction pattern of the as-made sample of SSZ-51. Peaks in the low-angle range are labeled with their respective *hkl* indices. Note the presence in this sample of peaks due to berlinite (the AlPO analogue of quartz, see Figure 1). The presence of peaks from berlinite does not affect the results from XRD as the multiple phase analysis is relatively straightforward. As the material is heated to 300 °C, there are only slight changes in the XRD pattern. However, at 400 °C there are dramatic changes in both the peak positions and intensities as the template and fluoride are removed from the structure. The shifts are readily apparent in the positions of the 110, 200, and 310 reflections. The

(20) (a) Olivier, J. P. *J. Porous Mater.* **1995**, *2*, 9. (b) Olivier, J. P. *Carbon* **1998**, *36*, 1469.

high-temperature XRD pattern can be indexed by a *C*-centered monoclinic cell with lattice parameters of $a = 22.471$ Å, $b = 13.735$ Å, $c = 14.052$ Å, $\beta = 98.5°$ (as verified by a LeBail profile fit). This indicates that there has been no change of symmetry of the material during calcination. While the other lattice parameters show little change, the *a* lattice parameter increases by 3.3%. This change seems mostly due to the relaxation of the framework as the fluoride bonds with the framework are broken. Simple energy minimizations to optimize the framework atom positions and unit cell parameters of the calcined material ($a = 22.724$ Å, $b = 13.718$ Å, $c = 14.019$ Å, $\beta = 99.2°$) are consistent with the observed parameters.

After 400 °C, there is little variation in the pattern due to structural changes in SSZ-51. At 800 °C the XRD pattern shows some disparity near 9.43 and 11.98° 2θ, but this is likely due to structural changes in the berlinite, which exhibits a phase transition near 600 °C.

The good thermal stability of SSZ-51 is quite surprising in that the material survived calcination to 800 °C while retaining a quite crystalline structure. This is at odds with the room-temperature XRD pattern, which shows a distinct loss of crystallinity. This change in XRD pattern must then be due to the rehydration of the framework rather than any inherent thermal instability of the framework. On leaving the calcined SSZ-51 in moist air for a day, the broad diffraction pattern is again recorded (Figure 11). However, on heating the sample to 100 °C, the diffraction pattern reverts to that which we expect for a highly crystalline sample of SSZ-51, with most of the expected reflections from the unit cell distinctly visible. It would appear that the rehydration process affects the crystallinity of the SSZ-51 framework markedly. A similar effect is seen in the thermal treatment of SAPO-40,[19] which has the closely related AFR framework structure described above. Once again, the structure of the framework is grossly changed by the addition of water at room temperature, removing the long-range order in the structure and producing an X-ray diffraction containing broad Bragg peaks. In both SSZ-51 and SAPO-40 this behavior is probably closely linked to the addition of water to the framework aluminum atoms, producing 5- and perhaps 6-coordinated aluminum atoms and so distorting the structure away from that found for the dehydrated framework.

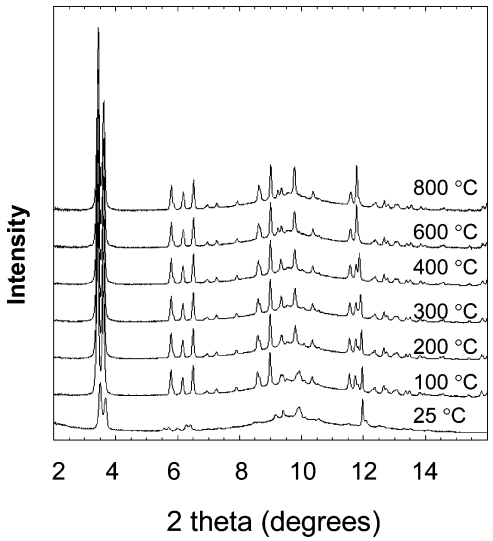

Figure 11. X-ray diffraction patterns of calcined SSZ-51 during dehydration.

Concluding Remarks

A new aluminophosphate zeolite material, SSZ-51, has been prepared hydrothermally using fluoride ions as a mineralizing agent. The structure is closely related to a previously discovered aluminophosphate zeolite, AFR. The synthesis of the new framework illustrates once again the utility of the fluoride method for the preparation of new materials in zeolite science.

Acknowledgment. R.E.M. thanks the Engineering and Physical Sciences Research Council (U.K.) for access to the synchrotron radiation facility at Daresbury and the Royal Society for provision of a University Research Fellowship. We also thank Son-Jong Hwang for his assistance. The Caltech solid state NMR facility was supported by the National Science Foundation under Grant No. 972420. Access to the National Synchrotron Light Source, Brookhaven National Laboratory, is supported by the U.S. Department of Energy, Division of Materials Sciences and Division of Chemical Sciences.

Supporting Information Available: X-ray crystallographic data (CIF). This material is available free of charge via the Internet at http://pubs.acs.org.

CM0353005